armadillo, *bazooka*, and *stardust* Are Critical for Early Stages in Formation of the zonula adherens and Maintenance of the Polarized Blastoderm Epithelium in *Drosophila*

H.-Arno J. Müller and Eric Wieschaus

Department of Molecular Biology, Princeton University, Princeton, New Jersey 08540

Abstract. Cellularization of the *Drosophila* embryo results in the formation of a cell monolayer with many characteristics of a polarized epithelium. We have used antibodies specific to cellular junctions and nascent plasma membranes to study the formation of the zonula adherens (ZA) in relation to the establishment of basolateral membrane polarity. The same approach was then used as a test system to identify X-linked zygotically active genes required for ZA formation. We show that ZA formation begins during cellularization and that the basolateral membrane domain is established at mid-gastrulation. By creating deficiences for defined regions of the X chromosome, we have identified genes that are required for the formation of the ZA and the generation of basolateral membrane polarity. We show that embryos mutant for both *stardust* (*sdt*) and *bazooka* (*baz*) fail to form a ZA. In addition to the failure to establish the ZA, the formation of the monolayered epithelium is disrupted after cellularization, resulting in formation of a multilayered cell sheet by mid-gastrulation. SEM analysis of mutant embryos revealed a conversion of cells exhibiting epithelial characteristics into cells exhibiting mesenchymal characteristics. To investigate how mutations that affect an integral component of the ZA itself influence ZA formation, we examined embryos with reduced maternal and zygotic supply of wild-type Arm protein. These embryos, like embryos mutant for both *sdt* and *baz*, exhibit an early disruption of ZA formation. These results suggest that early stages in the assembly of the ZA are critical for the stability of the polarized blastoderm epithelium.

One of the major challenges in epithelial cell biology is to determine the mechanisms underlying the biogenesis of epithelia and the dynamic cell rearrangements that occur in epithelial tissues during morphogenesis. Epithelial cells have a polarized organization, i.e., they exhibit an apical-basolateral polarity with respect to the cytoskeleton and the distribution and transport of certain membrane proteins and intracellular organelles (Simons and Fuller, 1985; Rodriduez-Boulan and Nelson, 1989; Nelson, 1992; Mays et al., 1994; Eaton and Simons, 1995). A set of specific cell contacts, the junctional complex, is found at the border between apical and basolateral plasma membrane domains (Staehelin, 1974; Lane and Skaer, 1980). Although junctional complexes of vertebrate and invertebrate epithelia differ, one cellular junction, the zonula adherens (ZA)[1], is present in both types of epithelia (Woods and Bryant, 1993; Kirkpatrick and Peifer, 1995). The ZA belongs to a family of actin-associated cell junctions called adherens junctions (Geiger and Ginsberg, 1991). The ZA is thought to provide an adhesive and contractile system that is important for the maintenance and the morphogenesis of epithelial tissues (Garrod and Collins, 1992). The functional center of the ZA is established by the cadherin-catenin based homophilic adhesion system. Cadherins are transmembrane glycoproteins which mediate Ca^{2+}-dependent cell adhesion and interact through their cytoplasmic domains with α-, β-, and γ-catenin, and $P120^{cas}$ (Magee and Buxton, 1991; Reynolds et al., 1994). The binding of cadherin to catenins mediates an interaction with the actin cytoskeleton and is essential for the adhesive function of cadherins (Kemler, 1993; Ranscht, 1994). Cadherins are not only an integral component of the ZA, but they are also crucial for the biogenesis of epithelial tissues in vitro and in vivo (McNeill and Nelson, 1992); they are key regulators for inducing surface polarity, maintaining epithelial cell shape and polarity, and suppressing invasive behavior of cells (Mege et al., 1988; McNeill et al., 1990; Birchmeier et al., 1993; Takeichi, 1993). At the cytoplasmic surface of the ZA, the actin cytoskeleton forms a continuous apical belt that inserts into a dense

Please address all correspondence to E. Wieschaus, Department of Molecular Biology, Princeton University, Princeton, NJ 08540. Tel.: (609) 258-5401. Fax: (609) 258-1547.

1. *Abbreviations used in this paper*: Arm, Armadillo; *arm*, armadillo (gene); baz, bazooka; Crb, Crumbs; *crb*, crumbs (gene); fog, folded *gastrulation*; NT, neurotactin; PY, phosphotyrosine; SAJ, spot adherens junctions; sdt, stardust; TEM, transmission-electron microscopy; ZA, zonula adherens.

cytoplasmic plaque which is composed of a variety of proteins, including the catenins, vinculin, and α-actinin (Tsukita et al., 1992).

Although much has been learned about the structure and the molecular components of the ZA, the mechanisms that lead to its assembly and disassembly are poorly understood. Cell culture studies suggest that biogenesis of the ZA may involve the successive assembly of a higher-order cadherin-cytoskeletal complex and the phosphorylation of its components (Gumbiner et al., 1988; Tsukita et al., 1992; Naethke et al., 1993; McNeill et al., 1993). Embryos have provided an additional model system to study the establishment of epithelial polarity (For review see Shiel and Caplan, 1995*b*). In mouse, chicken, frog, and fish embryos epithelialization commences soon after or even during cleavage (Lentz and Trinkaus, 1967; Trelstad et al., 1967; Collins and Fleming, 1995; Müller and Hausen, 1995). In mouse embryos, the formation of epithelial cell polarity and of cellular junctions has been studied in great detail, and a central role of E-cadherin in these processes has been established (Vestweber and Kemler, 1984; Fleming and Johnson, 1988; Fleming et al., 1993; Larue et al., 1994; Riethmacher et al., 1995).

The ZA of *Drosophila* resembles its mammalian counterpart structurally, and many of its molecular components are conserved (Peifer, 1995). The *Drosophila* homologues of the cadherin-catenin system are known as *D*E-cadherin, *D*α-catenin, and Armadillo (β-catenin) (Peifer and Wieschaus, 1990; Oda et al., 1993, 1994). The phenotypes for loss of the *D*E-cadherin and *D*α-catenin genes have not been described. The function of *arm* as a segment polarity gene has been well established (Peifer, 1995). However, the function of Arm in the ZA of embryos has been difficult to analyze because of its strong maternal component of expression. Although it is most likely that Arm, like its vertebrate homologue β-catenin, is critical for cell adhesion, this function has thus far only been demonstrated for oogenesis (Peifer et al., 1993). Analysis of two other genes, *crumbs* (*crb*) and *stardust* (*sdt*), revealed that they are involved in the biogenesis of epithelial cell polarity (Knust et al., 1993; Knust, 1994). The *crb* gene encodes an EGF-like transmembrane protein that is expressed on the apical membrane domain of ectodermally derived epithelia (Tepass et al., 1990). Crb has been implicated in apical protein targeting, and expression studies have further shown that Crb is able to confer an apical character to a plasma membrane domain (Wodarz et al., 1993, 1995). *sdt* or *crb* mutant embryos have similar phenotypes characterized by a late disruption of ectodermally derived epithelia. The mislocalization of Crb protein in *sdt* mutant embryos suggests that *sdt* might function already early in development (Tepass and Knust, 1993).

The first epithelium in the *Drosophila* embryo is formed immediately before gastrulation. The preceding 13 cleavage divisions occur without cytokinesis, thus giving rise to a syncytial blastoderm with the nuclei closely aligned in the peripheral cytoplasm of the embryo. During the next cleavage division (cycle 14), cytokinesis takes place in a complex process called cellularization (Schejter and Wieschaus, 1993). The formation of cell membranes begins with the generation of cleavage furrows from the periphery of the embryo in radial direction. New plasma membranes are assembled until a monolayered cell sheet has formed that shares many features with epithelial cell monolayers, including epithelial cell junctions and polarized membrane transport (Mahowald, 1963; Sanders, 1975; Eichenberger-Glinz, 1979; Tepass and Hartenstein, 1994; Shiel and Caplan, 1995). Although spotlike adherens junctions are already formed early during cellularization, transmission-electron microscopy indicates that the establishment of the continuous ZA is accomplished only later in development (Tepass and Hartenstein, 1994).

We have used antibodies to study the assembly of the ZA and the establishment of basolateral membrane polarity in early embryos and to screen for mutants that affect these processes. The distribution of junctional and basolateral markers in the wild type indicates that the apical-basolateral axis of the emerging cells is established during cellularization. We show that two loci, *stardust* (*sdt*) and *bazooka* (*baz*), can account for most, if not all, of the early effects of X-chromosomal zygotically active genes on ZA formation. Moreover, we demonstrate that the phenotype of *sdt baz* double mutant embryos resembles that of embryos missing normal maternal contribution of Arm. The failure to assemble an early precursor stage of the ZA leads to lack of basolateral membrane polarity and is accompanied by conversion of the blastoderm epithelium into a mesenchymal cell mass during gastrulation. These results suggest that ZA formation is essential for the structural integrity of the blastoderm epithelium.

Materials and Methods

Fly Stocks and Generation of Germ-Line Clones

nullo-X; *1E* embryos were produced using the stock *C(1)DXywf*; *1E* described by Simpson and Wieschaus (1992). *1E* is an autosomal transgene that carries a wild-type copy of *nullo*, necessary for normal cellularization. Stocks carrying chromosomal translocations were obtained from the Bowling Green Stock Center (Bowling Green, OH). The segregation of the translocation chromosomes in males was tested by mating them to *C(1)DXywf*; *1E* females and analyzing the phenotypes by observation of living embryos. The segregants can be easily identified by the presence or absence of the *folded gastrulation* (*fog*) phenotype (*fog* is located in 20 A3-B4) (for reference see Wieschaus and Sweeton, 1988).

sdt baz double mutants were made with the following alleles: sdt^{XN05}, sdt^{XP96}, baz^{YD97}, and baz^{Xi106} (Wieschaus et al., 1984). The stocks were ranked according to the severity of the cuticle phenotype, and sdt^{XN05} baz^{YD97} (named *22ND*) was chosen for additional experiments because it showed the strongest phenotype. The *22ND* double mutant embryos showed a substantial variation with respect to the developmental stage when abnormalities were first observed at the gross morphological level. We established stocks in which the *22ND* chromosome is maintained over a balancer that contains a *lacZ*-fusion transgene: *FM7 [ftz::lacZ]*. Since the only class of embryos from this stock that is negative for β-galactosidase (βgal) expression is the hemizygous mutant class (*22ND/Y*), we were able to assign the variety of late phenotypes observed to the hemizygous mutant condition. In contrast to the single mutant alleles, most of the double mutant embryos (~86% of the *22ND/Y* embryos) did not produce any detectable cuticle (the residual showed only some small cuticular fragments, a phenotype that was much stronger than in *sdt* single mutants). In addition, 15–20% of the embryos of the *22ND* stock showed wild-type cuticle differentiation, but did not hatch, suggesting that *sdt baz* has a weak penetrant dominant effect. In experiments involving single mutants the alleles sdt^{XP96} and baz^{Xi106} were used.

Germ-line clones were produced using the FLP-DFS system (Chou and Perrimon, 1992). arm^{XP33} *FRT101/FM7* females were mated with $Fs(1)ovo^{D1}$ *FRT 101/Y*; *hs-flp-F38* males. sdt^{XP96} *FRT18D/FM7* or baz^{Xi106} *FRT18D/FM7* females were mated with $Fs(1)ovo^{D2}$ *FRT18D [w+]/Y*. Mitotic recombination was induced in 2nd and 3rd instar larvae by activation of the

flipase transgene by heat shock. Females from this progeny were collected as virgins and mated with *FM7 [ftz::lacZ]/Y* males in order to discriminate hemizygous null mutants from heterozygotes. The Oregon-R stock served as wild-type control.

Immunocytochemistry

Embryos were collected on yeast-coated apple juice plates. Since staging of severely abnormal embryos is difficult, blastoderm-stage embryos were selected by observation under halocarbon oil (Sigma Chem. Co., St. Louis, MO), and a batch of synchronized embryos (typically about 200) was then further processed. Embryos were dechorionated by 1.5 min incubation in commercial bleach and fixed using two different protocols. For NT and Arm staining, embryos were fixed according to the heat-methanol protocol (Miller et al., 1989). Briefly, dechorionated embryos were incubated in a hot Triton X-100 (0.03%) – NaCl (0.4%) solution (TNS) for 30 s, and then quickly cooled by addition of excess chilled TNS. Vitelline membranes were removed by shaking the embryos vigorously in a mixture of heptane and methanol (1:1). This fixation procedure highlights the localization of Arm in the ZA that would be otherwise obscured by the strong cytoplasmic component of Arm; Arm is present as a soluble pool in the cytoplasm and in a membrane-bound pool at the plasma membrane. The heat-methanol fixation procedure results in extraction of most of the cytoplasmic Arm; however, it maintains the plasma membrane–bound pool (Peifer et al., 1994). For localization of phosphotyrosyl epitopes, dechorionated embryos were fixed in a solution of modified Stefanini's fixative and heptane (1:1) (modified Stefanini's: 4% formaldehyde, 75 mM Pipes, pH7.4, 15% of saturated picric acid solution). After 30 min of fixation on a rockerplate, the fixative was removed and replaced by methanol to remove vitelline membranes. After either fixation, embryos were stored in methanol at −20°C. For immunolabeling, embryos were transferred into PBS-0.5% Tween (PBT). Nonspecific binding was blocked by preincubation in 10% BSA in PBT, and antibody incubations were performed in 1% BSA in PBT.

The antibodies used were (*1*) rabbit anti-Arm antibody (N2), affinity purified at 1:100 (Riggleman et al., 1990); (*2*) mouse anti-neurotactin (BP106), tissue culture supernatant at 1:5 (Hortsch et al., 1990; the hybridoma supernatant was obtained from the Developmental Studies Hybridoma Bank, Iowa City, IA); (*3*) mouse anti-phosphotyrosine (PY20; Transduction Laboratories, Lexington, KY), at 5 μg/ml; (*4*) rabbit anti-βgal affinity purified (Vector Laboratories, Burlingame, CA) at 1:1,000; (*5*) goat anti–mouse TRITC (5 μg/ml; Boehringer Mannheim Biochemicals, Indianapolis, IN); (*6*) goat anti–rabbit FITC (5 μg/ml; Boehringer); (*7*) goat anti–mouse Cy3™ (3 μg/ml; Jackson Immunoresearch, West Grove, PA); and (*8*) goat anti–rabbit biotin (1:500; Vector). All secondary antibodies were preabsorbed by overnight incubation with heat-methanol fixed embryos. For immunofluorescence, stained embryos were mounted either in AquaPolymount (Polysciences Inc., Warrington, PA) or Mowiol containing DABCO (1,4-diazabicyclo[2.2.2]octane) as an anti-bleaching agent and observed under an MRC 600 confocal microscope (BioRad Labs, Hercules, CA). Images were processed using Confocal Assistant (CAS™) and Adobe Photoshop™ software on a PowerMacintosh computer. Images were printed on a dye-sublimation printer (Codonics, Middleburg Heights, OH).

Transmission-electron Microscopy and Immunoelectron Microscopy

For structural analysis, embryos were hand selected and dechorionated as described above and fixed in 1:3.5 mixture of 25% glutaraldehyde in 50 mM sodium cacodylate buffer pH 7.4 and heptane for 15 min at room temperature. The vitelline membrane was then removed manually under 2% glutaraldehyde in 50 mM sodium cacodylate buffer, pH 7.4, and transferred into a mixture of 1% osmium tetroxide, 2% glutaraldehyde, and 50 mM sodium cacodylate buffer, pH 7.4, and fixed in this mixture for 2 h on ice. After washing in 100 mM sodium cacodylate buffer, pH 7.4, the embryos were postfixed in 1% osmium tetroxide in 50 mM sodium cacodylate buffer, pH 7.4, for 2 h on ice. After en bloc contrasting in 2% uranyl acetate, the specimens were dehydrated in EtOH and propylenoxide and embedded in Embed 812 (Electron Microscopic Sciences, Fort Washington, PA). Serial thin sections were stained with 2% uranyl acetate and lead citrate.

For immunoelectron microscopy embryos were fixed in the modified Stefanini's fixative as described above. Dehydration after the PLT protocol and deep temperature embedding in Lowicryl K4M was performed as described previously (Müller and Hausen, 1995). Thin sections were stained with mouse anti-phosphotyrosine (PY20; Transduction Laboratories) and goat anti–mouse IgG conjugated with 12-nm colloidal gold particles (Jackson Immunoresearch), both at 5 μg/ml. Sections were postfixed with 2% glutaraldehyde in PBS, treated with 2% reduced osmium tetroxide for 30 min to enhance contrast and stained with 2% uranyl acetate and lead citrate.

Thin sections were observed under a JEOL 100C transmission electron microscope at 80 kV. Negatives were scanned with a UMAX UC1260 scanner and processed using Adobe Photoshop™ 3.0 software.

Scanning Electron Microscopy

The *22ND/FM7[ftz::lacZ]* stock was used to discriminate mutant from wild-type embryos. Hemizygotes represent the only embryos from this stock that do not stain with anti-βgal antibodies. As a control, Oregon R embryos were treated in a similar manner. First, embryos were fixed in 4% formaldehyde in PBS and heptane (1:1) for 45 min. After removing the vitelline membrane in heptane/methanol, the embryos were stained for βgal as described using the ABC-detection kit (Vector). Mutant embryos and normal embryos were separated and processed for SEM (βgal staining was unequivocally recognizable at midcellularization stages). The embryos were postfixed in 1% osmium tetroxide in PBS for 2–4 h and en bloc contrasted with 2% uranyl acetate for 2 h. Dehydration in a rising ethanol series was followed by infiltration with PELDRI II (Ted Pella, Polysciences Inc.) for a total of 3 h. PELDRI was solidified on ice and allowed to sublimate overnight. Embryos were mounted on double-stick carbon tape and aluminum tape on SEM stubs (Polysciences Inc.). After sputtering with gold-palladium in a Denton Desk II sputter, the specimens were observed and photographed in a JEOL 840 SEM at 5 kV.

Results

Formation of the ZA and Basolateral Membrane Identity in the Wild-type Embryo

Adherens junctions not only contain large amounts of cadherin-catenin complexes, but are also characteristically enriched for phosphotyrosine (PY) epitopes. Consistent with earlier studies in vertebrate and insect epithelia, we found that in embryos PY epitopes were localized to the electron-dense cytoplasmic plaques of the ZA (Fig. 1) (Takata and Singer, 1988; Tsukita et al., 1991; Woods and Bryant, 1993). Optical sections through stained wild-type embryos of different stages revealed that Arm and PY colocalize to a large extent (Fig. 2). Because Arm and PY are colocalized in the ZA, we used them as markers to demonstrate the formation of the ZA during embryogenesis.

In cellularizing embryos, Arm and PY are initially found along the lateral membranes and enriched at the tips of the cleavage furrows. A major redistribution of Arm and PY occurs during cellularization and early gastrulation. At mid-cellularization, staining becomes stronger on the apical aspect than in the more basal part of the lateral domain (Fig. 2, *A* and *B*). This staining pattern continues to change within the next 30 min of embryogenesis. By the end of cellularization, Arm and PY staining are strongly reduced at the basal part of the furrow. Only slightly later, within a period of ~10 min, Arm and PY become concentrated in discrete spots at the apical-lateral border of the ectodermal cell layer (see Fig. 3). At the end of gastrulation (stage 9), both antigens have accumulated in the apical-lateral cell contacts in the ectoderm, whereas only very little staining is present on the basolateral membrane domain (Fig. 2, *C* and *D*).

We next sought to relate the dynamic changes in the distribution of the junctional markers to the generation of the

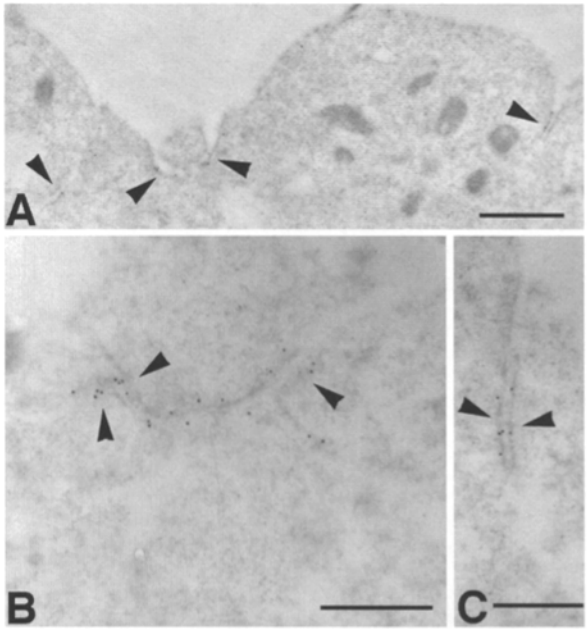

Figure 1. Immunoelectron-microscopic localization of PY. Ultrathin Lowicryl (K4M) sections of embryos (stage 13) were immunostained with anti-PY antibodies and a secondary antibody conjugated to 12-nm colloidal gold. A low power micrograph is shown in *A* (the arrowheads point at the electron dense region of the ZA). In high power micrographs (*B* and *C*) gold particles can be seen decorating the cytoplasmic plaque region of the ZA. *B* shows a slightly tangentially oriented section with ZAs of three adjacent cells. Bars: (*A*) 1 μm; (*B* and *C*) 0.5 μm.

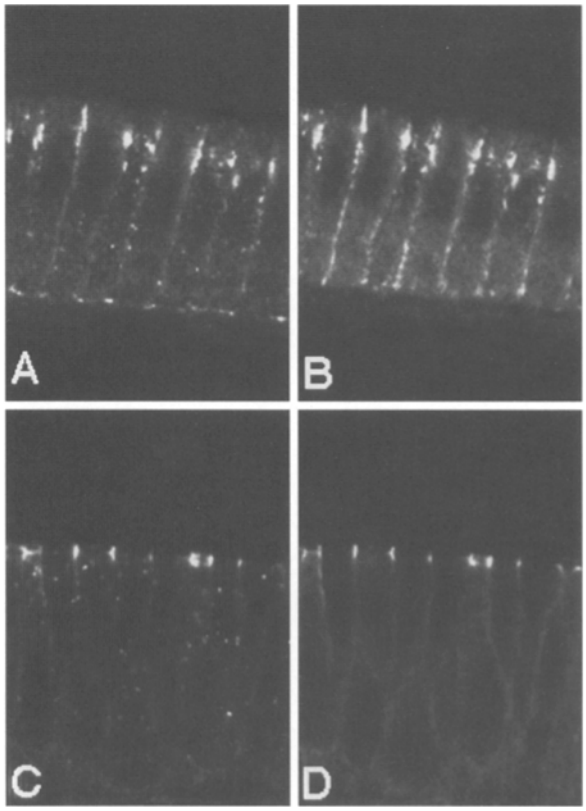

Figure 2. Double immunolabeling of phosphotyrosyl proteins (PY) and Armadillo (Arm) in blastoderm and gastrula embryos. Embryos at the cellularization stage (stage 5) (*A* and *B*) and at the extended germ-band stage (stage 9) (*C* and *D*) were simultaneously whole-mount stained with antibodies against PY (*A* and *C*) and Arm (*B* and *D*), and analyzed by confocal microscopy. The panels *A* and *B* and *C* and *D* represent pairs of the same region using different filter sets according to the secondary antibody conjugate used. The only observed difference between PY and Arm labeling was in the base of the furrow tips during cellularization. Bar, 10 μm.

polarized blastoderm epithelium. To study the development of the ZA and the establishment of the basolateral membrane domain simultaneously, we performed double immunolabeling using antibodies against Arm and antibodies against the membrane protein neurotactin (NT) (Hortsch et al., 1990). At the beginning of cellularization, when Arm is localized at the tip of the cleavage furrows, NT staining is punctate and distributed all over the peripheral cytoplasm of the embryo (Fig. 3 *A*). As the cleavage furrows progress to the level of the nuclei, NT staining becomes more concentrated in the cortical region of the embryo, but is still not observed in the forming membranes (Fig. 3 *B*). NT first appears in the nascent membranes when the furrow tips have passed the nuclei. At this stage, Arm and NT staining overlap to a great extent in the lateral region of the forming membranes (Fig. 3 *C*). The major redistribution of Arm to the apical region precedes the changes in NT distribution (Fig. 3 *D*). NT remains in the lateral region both apically and basally to the Arm spots demarcating the localization of the emerging ZA (Fig. 3 *E*). When germ-band extension begins at stage 7, the final pattern of Arm and NT staining is reached: Arm is concentrated at the border of the apical and lateral membrane domains, and NT is present basolaterally, but no longer found apical to the ZA (Fig. 3 *F*).

These results suggest that the ZA and the basolateral membrane domain are established successively. The early redistribution of Arm protein suggests that ZA formation in the apical region of the nascent membranes begins during cellularization. The basolateral membrane protein NT maintains some localization apical to the emerging ZA until later in gastrulation. At this time the emerging ZA reaches its final position and forms the border between the apical and the basolateral membrane domain.

X-Chromosomal Zygotic Transcription Is Required for ZA Formation

To identify genes that are required for the formation of the ZA and basolateral membrane polarity, we used a genetic protocol established earlier to identify genes that are essential for cellularization (Wieschaus and Sweeton, 1988). The general strategy of this experiment is to create large deficiencies over the X chromosome using compound 1 stocks and chromosomal translocations. In compound 1 females, the two X chromosomes are attached to each other and segregate during meiosis against a Y chromosome. Therefore, a quarter of all embryos produced by a compound 1 stock inherit two Y chromosomes from their parents and are deficient for the entire X chromosome (*nullo-X* embryos) (Wieschaus and Sweeton, 1988). Because the X chromo-

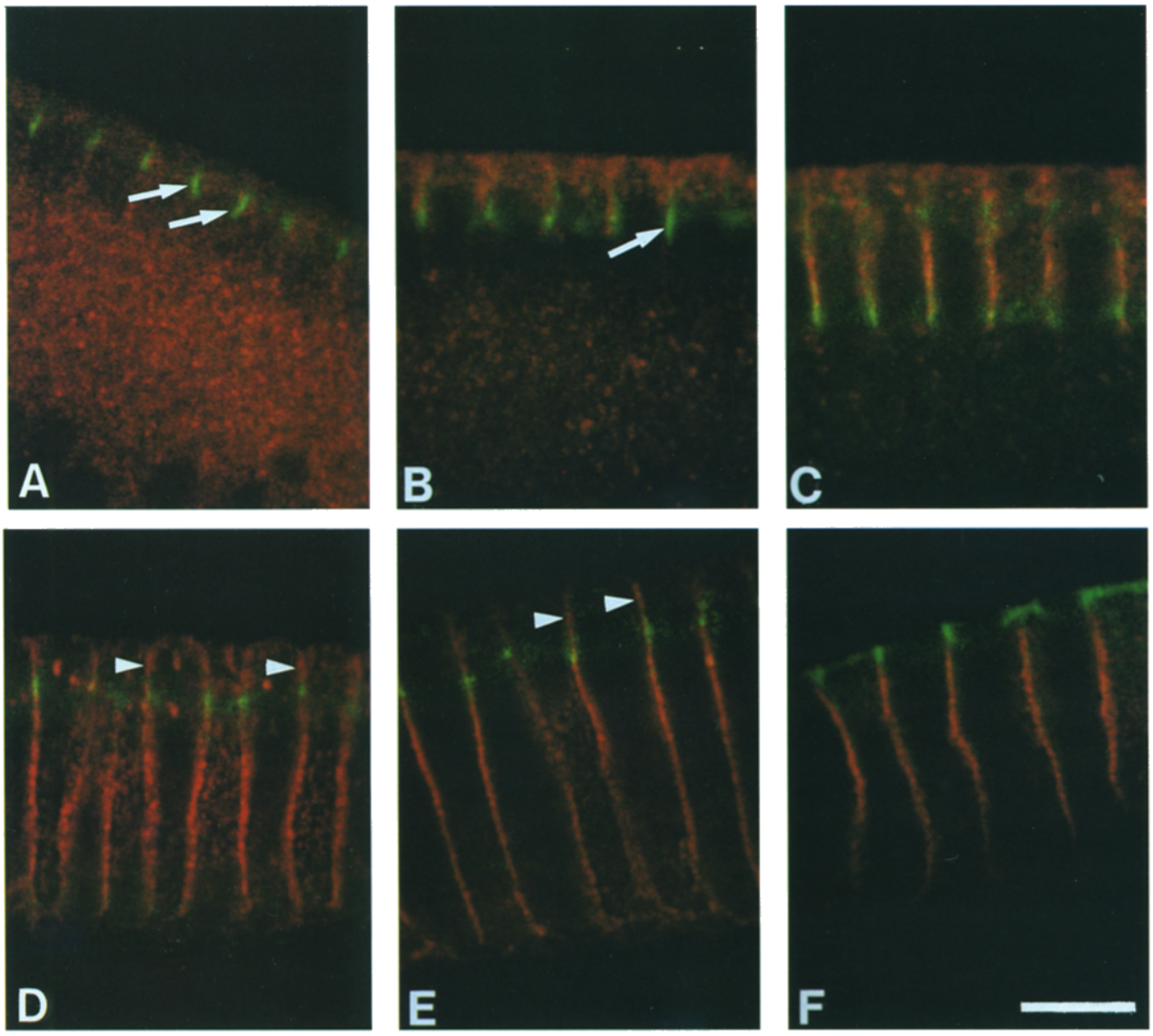

Figure 3. Double immunolabeling of Neurotactin (NT) and Arm during cellularization and gastrulation. Confocal sections were taken from whole-mount stained embryos using the anti-NT antibody (*red*) and the anti-Arm antibody (*green*), simultaneously. Single images were taken and merged using the BioRad COMOS 6.03 software. *A–D* show progressing stages through cellularization in cycle 14 (stage 5). Note staining of Arm in the early advancing furrows (*arrows*) in *A* and *B*. Sections through early (stage 6) and mid- (stage 8) gastrulation embryos are shown in *E* and *F*, respectively. Arrowheads in *D* and *E* point to apical localization of NT relative to the emerging ZA. Bar, 10 μm.

some carries a gene essential for cellularization, *nullo* (Simpson and Wieschaus, 1990), we used a compound 1 stock that harbors an autosomal *nullo* transgene, *1E*, and allows for normal cellularization in *nullo-X* embryos (*C(1)DXywf; 1E*) (Simpson and Wieschaus, 1992). This situation allowed us to study the requirements of X-linked zygotic gene activity for formation of the ZA in the embryo.

Embryos from the stock *C(1)DXywf; 1E* were staged and fixed as they finished germ-band extension at embryonic stage 9. In comparison to their wild-type siblings, *nullo-X;1E* embryos did not show any recognizable concentration of maternally provided Arm at cell contacts of the outer cells instead, Arm is distributed more or less uniformly along the surface of the cells (Fig. 4, *A* and *B*). Embryos that lack X-linked zygotic transcription do not localize Arm at apical-lateral cell contacts in the outer cell layer; this result suggests a failure in the establishment of the ZA. The lack of the ZA in *nullo-X; 1E* embryos was confirmed by failure of PY localization and by TEM analysis (Sweeton, D., and E. Wieschaus, unpublished observations; see also Fig. 7).

To map the gene on the X chromosome responsible for the observed defect in ZA formation, we used a set of chromosomal translocations (Fig. 5). Meiotic segregation in the germline of males bearing *T(1;Y)* translocations results in the production of gametes that are either deficient for the proximal or the distal fragment of the X chromosome relative to the translocation breakpoint. When such

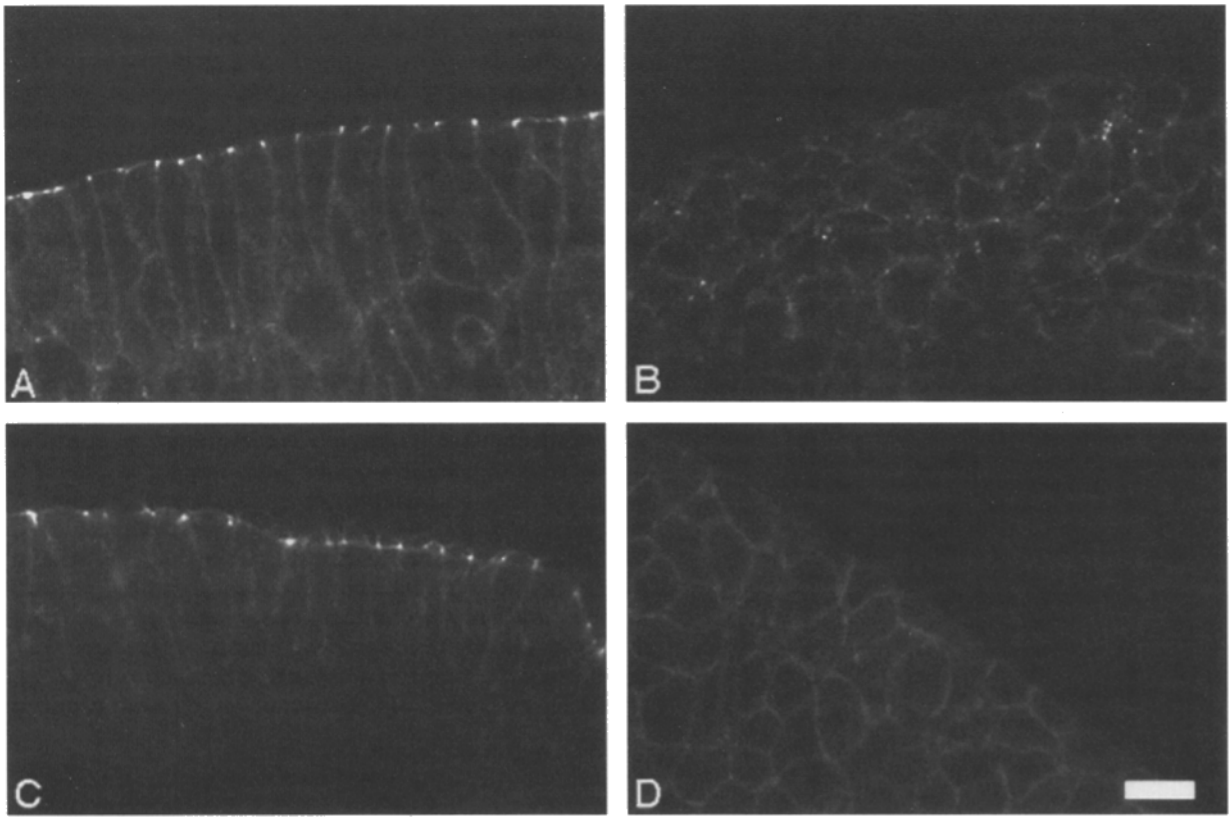

Figure 4. Arm localization in *nullo X; 1E* embryos and embryos obtained from a translocation cross using *T(1;Y)B17*. Embryos at the extended germ-band stage (stage 9) were fixed, stained for Arm, and observed under the confocal microscope. A wild-type pattern of Arm is seen in three quarters of the embryos from the compound 1; *1E* stock (*C(1)DXywf; 1E*) (*A*). In *nullo X; 1E* embryos the regular pattern of Arm localization in the outer cell layer is absent (*B*). When *C(1)DXywf; 1E* females are crossed to males bearing translocations of a part of the X chromosome to the Y chromosome (T(1;Y)), two classes of abnormal embryos, deficient for either the proximal or the distal part of the X chromosome, are obtained. An example of distal and proximal deficiency class embryos with respect to a breakpoint at 7C are shown in *C* and *D*, respectively. Only the proximal deficiency class (*D*) shows the abnormal ZA phenotype. Bar, 10 μm.

males are crossed to compound 1 females, 50% of the embryos are abnormal because they obtained a Y chromosome from the mother and either the distal or proximal fragment of the X chromosome from the father (see Wieschaus and Sweeton, 1988). The ZA phenotype occurred in embryos that lack either the region proximal of (chromosomal region) 7C or distal of 16F (Fig. 4, *C* and *D*; Fig. 5). Interestingly, in crosses using translocations that break either at 7F, 13E, or 15A, none of the deficiency classes of embryos showed the abnormal ZA phenotype. This observation led to the hypothesis that these embryos had to be missing two loci, one in 7C-F and one in 15A-16F, to produce the same defect in ZA formation observed in embryos that lack the entire X chromosome.

The nullo-X; 1E Phenotype Is Mimicked by a sdt baz Double Mutant

The chromosomal regions 7C-F and 15A-16F each contains a gene implicated in later epidermal differentiation: *stardust* (*sdt*; 7D10-7F2) and *bazooka* (*baz*; 15 D14-22). Mutations in these genes lead to a zygotic embryonic lethal phenotype, which in both cases is characterized by severe malformations or an absence of the embryonic epidermis (Wieschaus et al., 1984; Tepass and Knust, 1993). To test whether the combination of mutations in *sdt* and *baz* is the basis for the *nullo-X; 1E* phenotype, we established four double mutant combinations of different alleles of *sdt* and *baz*, and analyzed the development of mutant embryos and the phenotype of larval cuticles. The double mutant sdt^{XN05} baz^{YD97} (named *22ND*) showed the most severe phenotype and was selected for additional experiments (see Materials and Methods).

When cellularization is completed, embryos hemizygous for *22ND* fail to concentrate Arm in the apical region of the newly forming membranes. Arm is scattered in spots over the entire lateral membrane and overlaps with NT (Fig. 6 *A*). At the beginning of germ-band extension (stage 7), an apical concentration of Arm is still absent and some regions display loss of discrete Arm spots and complete mixing of junctional and basolateral membrane markers (Fig. 6 *B*). This early disruption of ZA formation is the same as observed in *nullo-X; 1E* embryos. At stage 9, when heterozygous control embryos have finished germband extension, the ZA is absent in the hemizygous mutant embryos and no apical-basolateral membrane polarity is established (Fig. 6 *C*).

The effect of the double mutant combination of *sdt* and *baz* on the formation of the ZA was confirmed by TEM analysis (Fig. 7). The fine structure of cell–cell adherens

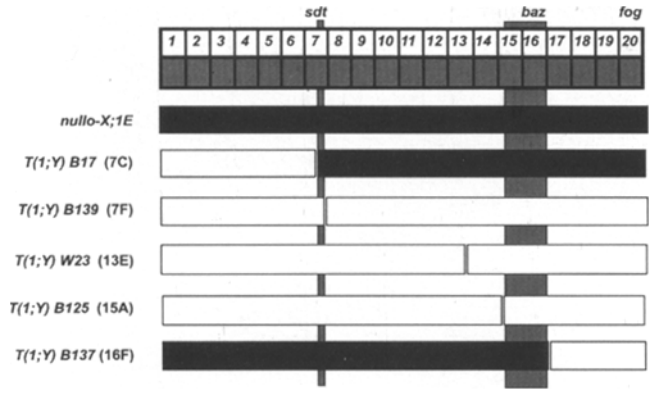

Figure 5. Scheme of the screen on the X chromosome using chromosomal translocations. The positioning along the X chromosome is indicated on the top of the panel (the location of the genes *sdt*, *baz*, and *fog* are indicated). The bars below represent different deficiencies that were generated using either the *C(1)DXywf; 1E* stock or crosses using males carrying different translocations as indicated on the left side of the bars (the translocation-breakpoints are indicated in parentheses) mated to *C(1)DXywf; 1E* females. The deficiency classes in a given cross can be distinguished by the early phenotype produced in the absence of the gene *folded gastrulation* (*fog*). Black bars indicate the presence of the abnormal ZA phenotype as shown in Fig. 3. Open bars represent the normal ZA development up to 1 h after the beginning of gastrulation. The shaded bars show the chromosomal regions that contain loci that are important for normal ZA development.

junctions can be described as regions of cell contact with constant intermembrane space and pronounced electron-dense cytoplasmic plaques (Fig. 7 *A*). In postgastrula embryos, adherens junction plaques are present at the apical-lateral boundary of the cells in the ectoderm indicating the presence of the ZA. In *sdt baz* mutant embryos the cytoplasmic plaques of the ZA are strongly reduced and often absent (compare Fig. 7, *A* and *B*).

In conclusion, *sdt baz* double mutant embryos exhibit the same early phenotype as *nullo-X; 1E* embryos, i.e., abnormal ZA formation and mislocalization of NT. A variable strength of late morphological abnormalities were observed in the *sdt baz* double mutants which had not been noticed in *nullo-X; 1E* embryos (see Materials and Methods). The more consistent late phenotype of *nullo-X; 1E* embryos most likely reflects deficiencies for other zygotically important X-linked genes which, like *folded gastrulation*, are essential for early development. In summary, we conclude that the X-linked zygotic defect in ZA formation is based on the absence of both *sdt* and *baz*.

The sdt baz Double Mutant Phenotype Is Stronger than sdt or baz Single Mutants

In contrast to the *sdt baz* double mutant phenotype, hemizygous *baz* single mutant embryos showed normal Arm and NT staining up to stage 10 of embryogenesis (i.e., 2 h later than abnormal ZA morphology was observed in hemizygous *22ND* embryos). Even at this rather late stage, the ZA was disordered only locally while large regions in the epidermis were still normal (Fig. 6, *D–F*). Similarly, *sdt* single mutant embryos exhibit abnormal ZA morphology only later in development as compared to the *sdt baz* double mutant (Fig. 8). In particular, in the early gastrula stage, when abnormalities in the *sdt baz* double mutant become first pronounced, the phenotype of *sdt* mutant embryos is almost identical to wild-type embryos (compare Fig. 8, *A* and *C*). Even after gastrulation (stage 9) large regions of the ectoderm form relatively normal ZAs (Fig. 8 *D*; compare also to Fig. 8, *H* and *I*).

The relatively weak zygotic phenotype of *baz* can be explained by a strong maternal component of expression of *baz* (Wieschaus and Noell, 1986). We therefore sought to analyze the ZA phenotype of embryos that lack both, maternal and zygotic *baz* activity by producing *baz* germ-line clones ("*baz* null"). Interestingly *baz* null embryos show a similar early disruption of ZA formation like the *sdt baz* zygotic double mutant (compare Fig. 8, *E*, *F*, and *G*). In particular, the concentration of Arm in the apical region of cell contact at the beginning of gastrulation is absent in both mutants (Fig. 8, *F* and *G*; see also Fig. 6 *A*). In addition to these early alterations in ZA formation, two morphological features of the mutant phenotypes are very similar: (*1*) When cellularization is completed, cell shapes in the mutant embryos are aberrant; instead of the highly columnar cell shape in the epithelium of wild-type embryos, the cells have irregular outlines and some appear bottle-shaped (Fig. 8, *F* and *G*, *lower panels*; see also Fig. 6 *A*). (*2*) The regular hexagonal pattern of Arm staining seen on the surface of wild-type embryos is distorted in the double mutants; the apical cell surfaces appear to vary in size, indicating that the apical domains are expanded in some cells and constricted in others (Fig. 8, *F* and *G*, *upper panels*). As expected, no ZAs are formed in *baz* null mutant embryos (Fig. 8, *H* and *I*, and *J*).

Cells of sdt baz Mutant Embryos Show Profound Changes in Their Morphology

The cells in late *sdt baz* mutant embryos fail to develop a ZA and to generate basolateral membrane identity as demonstrated by the disordered distribution of NT and Arm. The analysis of wild-type embryos suggested that ZA formation begins during cellularization with an increased concentration of Arm in the apical aspect of the newly formed lateral surface. Shortly after cellularization (stage 6), Arm concentrates strongly at the most apical region of lateral cell contact. The formation of this ZA precursor shortly after cellularization was already disturbed in *sdt baz* double mutant embryos. To investigate whether the emerging ZA serves any function at these stages of development, we analyzed the earliest alterations in cell morphology in *sdt baz* mutant embryos by scanning electron microscopy (SEM). At the beginning of gastrulation (stage 6), the surfaces of the cells in *sdt baz* mutant embryos are irregular in shape; some apices are large, some are small, and some cells have disappeared from the surface of the embryo altogether, creating holes in the epithelium (compare Fig. 9, *A* and *D*). In slightly older mutant embryos (stage 7), the characteristics of the epithelial cell surface are almost completely lost (Fig. 9, *B* and *E*). The loss of epithelial features of the cells appears as a complete conversion into cells with morphological characterisics of mesenchymal cells; the cells form processes and appear to spread over the embryonic surface (Fig. 9, *C* and *F*).

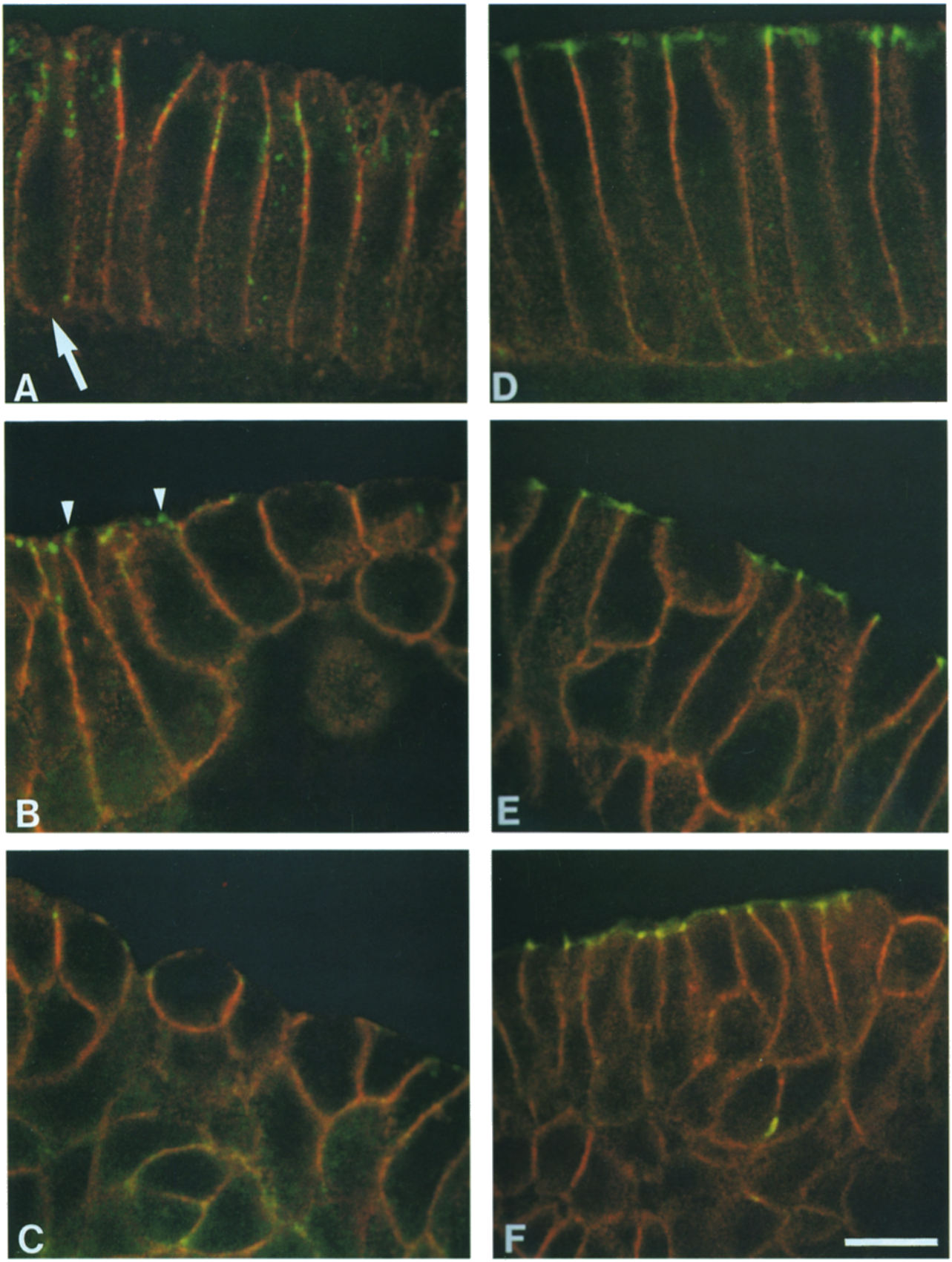

Figure 6. Armadillo and Neutrotactin double immunolabeling in zygotic *sdt baz* double mutant embryos (*A–C*) and zygotic *baz* mutant embryos (*D–F*). Embryos were staged as described in Materials and Methods, fixed, and stained for Arm (*green*) and NT (*red*). Merged images are depicted, and the yellow color indicates an overlap between the two antigens. An *sdt baz* embryo in early gastrulation is depicted in *A*. Note the scattered spotlike localization of Arm protein and the bottle-shaped cell (*arrow*). *B* and *C* show *sdt baz* mutant

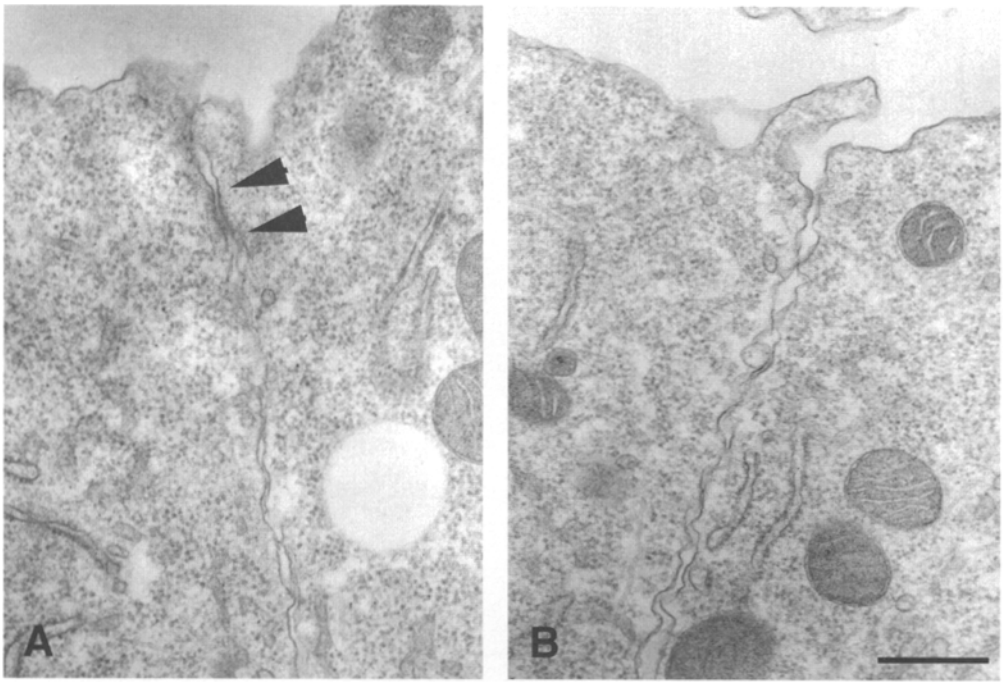

Figure 7. TEM analysis of *sdt baz* double mutant embryos. Postgastrula embryos were fixed and processed for TEM analysis. The apical-lateral contact area of adjacent ectodermal cells is compared between wild-type (*A*) and *sdt baz* double mutant (*B*) embryos. The arrowheads point to electrondense regions in the wild type indicating the presence of cytoplasmic plaques of adherens junctions. Bar, 0.5 μm.

The lack of normal zygotic transcription of both *sdt* and *baz* leads to profound alterations in cell shape which are first detected by the beginning of gastrulation (stage 6). Ultimately, the cells in the double mutant embryos undergo a complete conversion from an epithelial to a mesenchymal-like morphology. These results suggest that the emerging ZA is required for the integrity of the blastoderm epithelium shortly after cellularization is complete.

Embryos of arm^{XP33} Germ-Line Clones Show a Phenotype Similar to sdt baz Mutant Embryos

Arm is an integral component of the ZA (Peifer, 1993). The function of Arm in the ZA has been difficult to analyze because Arm is provided as a large maternal store, and thus abolishing the zygotic production of Arm does not lower its level enough to reveal effects on ZA formation. In addition, Arm is required for oogenesis, so the maternal contribution of Arm in the embryo cannot be easily eliminated using germ-line clones of *arm* null alleles (Peifer et al., 1993).

To study the role of Arm in ZA formation, we employed a moderate allele of *arm* (*arm^{XP33}*) which produces a COOH-terminal truncation of the Arm protein (Peifer and Wieschaus, 1990). The truncated protein reacts with our antibody and supports some of the adhesive function of the wild-type protein (Peifer et al., 1993; Peifer, 1995). Females bearing germ-line clones (glc) of *arm^{XP33}* lay some eggs, and embryos that receive wild-type *arm* alleles from their fathers develop normally (data not shown). Conversely, hemizygous *arm* embryos show only poor differentiation of the larval cuticle. Some of these embryos exhibit a cuticular phenotype very similar to the one observed in embryos zygotically mutant for *crb* or *sdt* (data not shown). Development of embryos derived from *arm^{XP33}* glcs was analyzed by video time-lapse recording. One rare class of mutant embryos showed very early defects, before and during cellularization. The majority of the mutant embryos, however, develop normally until early gastrulation. We concentrated our analysis on the latter class of mutant embryos. When gastrulation movements begin, the monolayered blastoderm epithelium becomes disordered, and some regions become multilayered in a manner similar to the *sdt baz* double mutant embryos. The late phenotype of the *arm* mutant embryos is also variable (Müller, H.-A.J., and E. Wieschaus, unpublished results).

To analyze the role of Arm in the formation of the ZA, embryos lacking the normal supplement of maternal and zygotic Arm (from *arm^{XP33}* glc) were fixed and stained with Arm antibodies. In early gastrulae (stage 7), only residual Arm staining is found in the region where the ZA formation normally occurs, although Arm is still present at low levels at the cell surfaces in a uniform pattern. In some regions of the embryos, Arm staining failed to concentrate at the sites where the ZA would normally form. It is these regions that undergo a change from a monolayer to a multilayer of cells (Fig. 10 *A*). In the majority of embryos, abnormal Arm staining was first observed in the ventral region of early gastrula embryos (data not shown). At later stages, apical Arm accumulation is absent at cell surfaces in the outer cell layer. Some spotlike staining of Arm remained, however, it was present in a more irregular pat-

embryos in an early gastrula (stage 7) and extended germ-band embryo (stage 9), respectively. Some apical-lateral localization can be seen even in stage 7 (arrowheads in *B*), but in stage 9 NT and Arm are completely intermingled. Sections through *baz* mutant embryos are depicted in *D* (stage 7), *E* (stage 9), and *F* (stage 10). Note that the polarized distribution of Arm and NT is unimpaired during gastrulation (*D* and *E*). Bar, 10 μm.

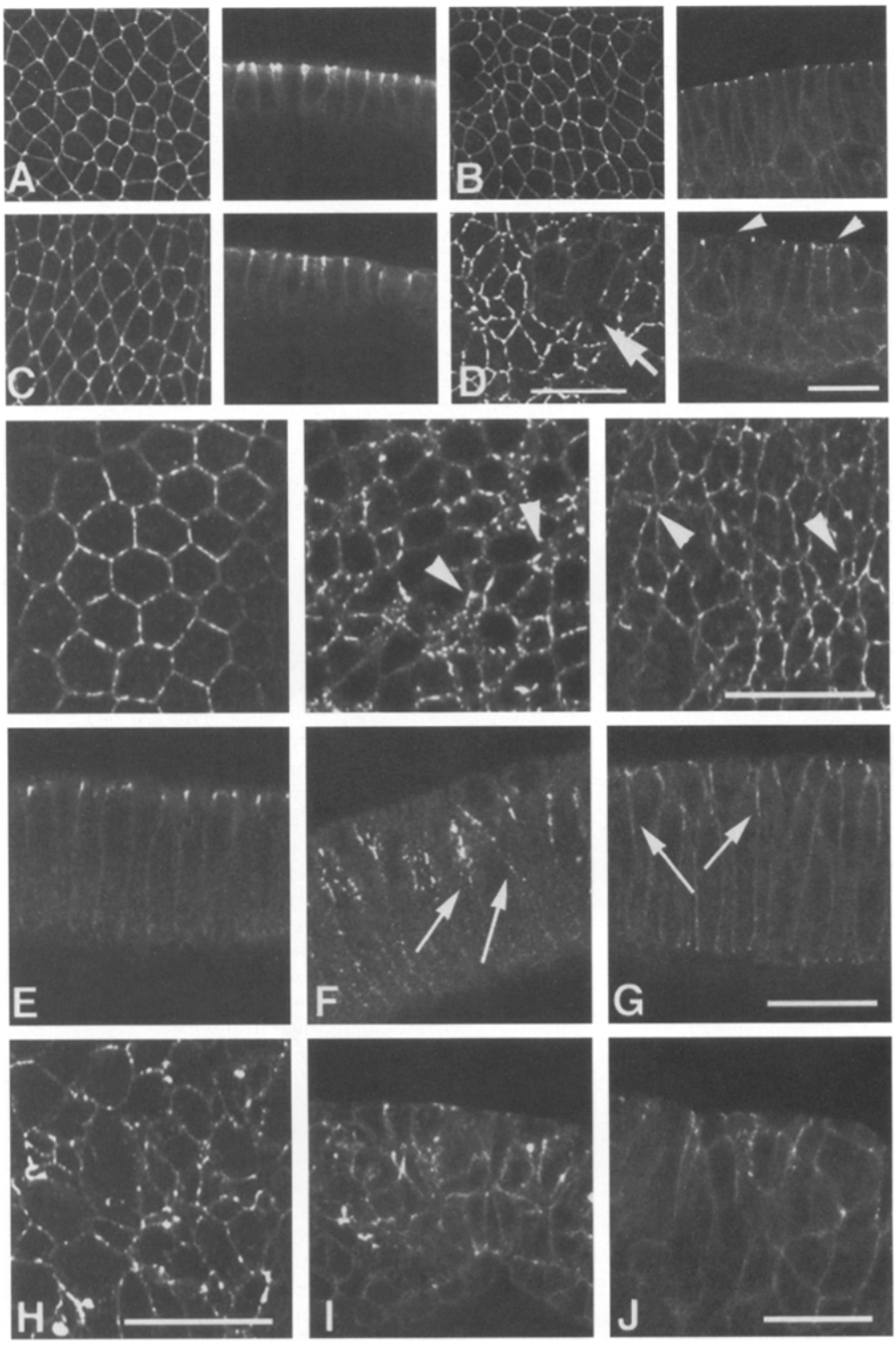

Figure 8. Comparison of the ZA phenotype of *sdt baz* double mutant embryos to *sdt* and *baz* single mutant embryos. Embryos were stained with anti-PY (*A* and *C*) or anti-Arm antibodies (*B* and *D–J*) and analyzed under the confocal microscope. (Since in early gastrula stages *sdt* mutant embryos are indistinguishable from wild-type embryos, the only way to unequivocally identify them as hemizygous mutant embryos is by using a marked balancer [*FM7[ftz::lacZ]*; see Materials and Methods]. Because the β-gal staining is only compatible in double labeling with the anti-PY marker, PY staining is shown for embryos in these early stages.) Wild-type embryos are compared to *sdt* null embryos early in gastrulation (stage 7) (*A* and *C*) and after gastrulation (stage 9) (*B* and *D*). In *A–D*, the left side of the panels shows a surface view and the right side of the panels shows an optical section. Note that at stage 7 the staining in *sdt* null mutant is very similar to wild type, whereas at stage 9 local disruptions in the honeycomb-like Arm surface pattern are visible (arrow in *D*; the arrowheads in *D* point to absence or irregular Arm-staining pattern in section). In *E*, *F*, and *G* early gastrula wild-type embryos (*E*) are compared to *sdt baz* double mutant embryos (zygotic) (*F*) and *baz* null embryos (*G*) obtained from females bearing *baz* germ-line clones (the upper panels show the surface and the lower panels show a representative cross section). Note that the cells in *sdt baz* double mutant embryos (*F*) and in *baz* null mutant embryos (*G*) exhibit an irregular surface pattern of Arm staining (arrowheads point at reduced apical surface areas) and a broader region of Arm staining on the lateral membrane (*arrows*). Postgastrula embryos of *sdt baz* double mutant embryos (*H*, surface; *I*, section) are compared to *baz* null mutants (*J*). Bars, 10 μm.

tern at outer and inner cell contacts (Fig. 10 *B*). Staining with anti-PY antibodies revealed essentially the same results, confirming that the loss of staining of the mutant Arm represents a loss in ZA structure (data not shown).

These experiments show that Arm is required for ZA formation. Moreover, embryos mutant for *arm* (derived from arm^{XP33} glc) and *sdt baz* double mutant embryos have very similar early phenotypes with respect to ZA formation.

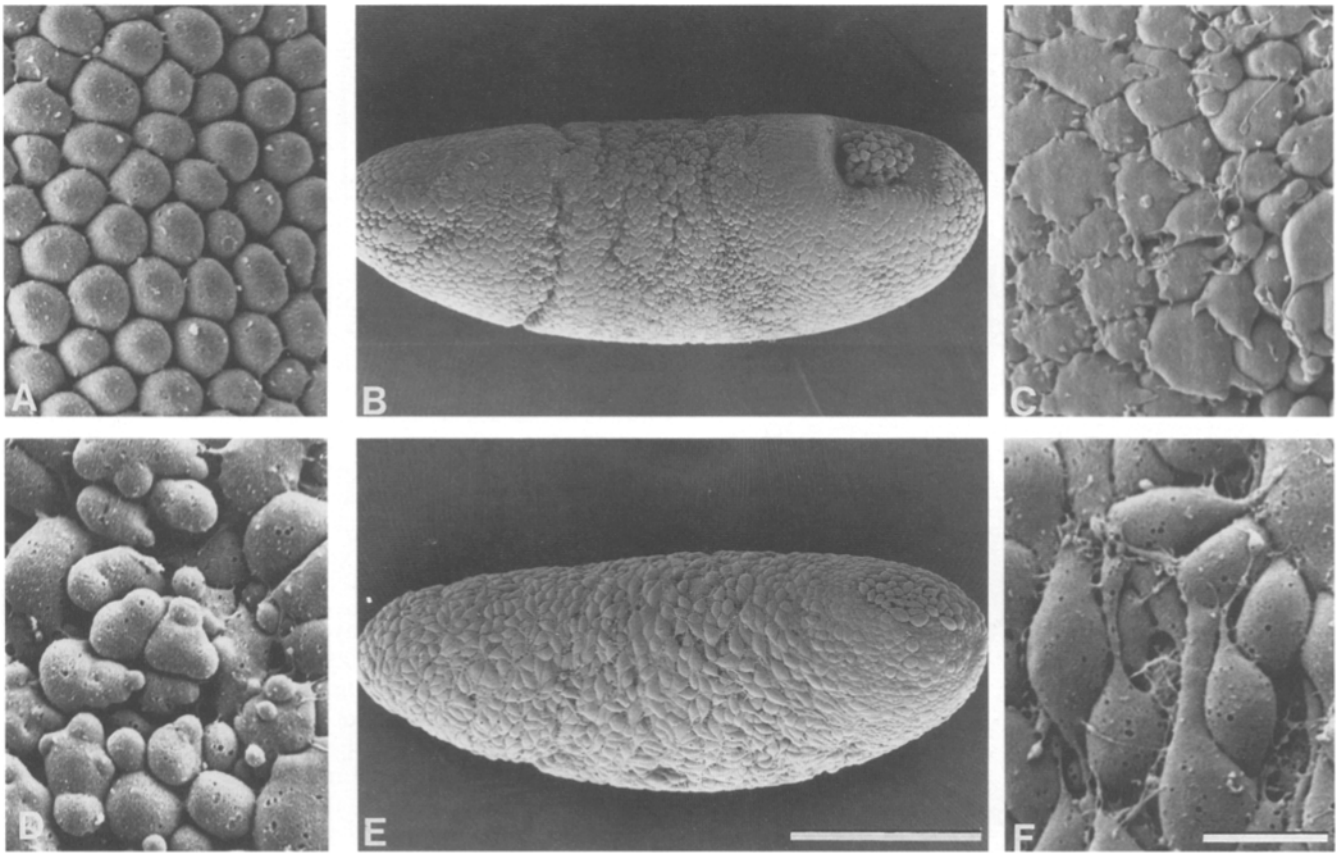

Figure 9. SEM analysis of early cell shape changes observed in *sdt baz* mutant embryos. Embryos from the stock *sdt baz/FM7[ftz::lacZ]* were fixed and stained for βgal to discriminate normal (*A*, *B*, and *C*) from hemizygous mutant (*D*, *E*, and *F*) embryos. The surface of early gastrulating embryos (stage 6 in *A* and *D*; and stage 7 in *B*, *C*, *E*, and *F*) is shown. Note the irregularly shaped cell apices in the mutant embryo in *D*. *B* and *E* show entire embryos to demonstrate that similar developmental stages are compared. *C* and *F* are higher power micrographs of the same embryos as shown in *B* and *F*. The holes in the membranes of the cells which are occasionally observed in the preparations are due to the rather gentle fixation conditions used to preserve βgal immunoreactivity. Comparison to stronger fixation protocols, however, revealed that the basic morphology of the cells is unimpaired regardless which protocol is used. Bars: (*A*, *C*, *D*, *F*) 10 μm; (*B* and *E*) 100 μm.

Discussion

Establishment of Apical-Basolateral Polarity in the Blastoderm Epithelium

During cellularization, Arm protein distribution changes dramatically from a basal to a more apical aspect of the lateral membranes. This progressive redistribution of Arm protein during cellularization indicates that, as the cells form, they already have an inherent apical-basal polarity. This polarity is also seen in the apical localization of the centrosomes, the apical-basal orientation of the microtubule network, and the high concentration of actin in the cortex of the blastoderm at the onset of cycle 14 (Schejter and Wieschaus, 1993). It is possible that the shift in the distribution of Arm reflects differential binding properties of the protein in the basal vs the apical region of the membrane, i.e., a reduced stability of Arm association with the plasma membrane at the furrow tip leads to decreasing amounts of Arm in this region by the end of cellularization. Alternatively, Arm localization may indicate the presence of preformed junctional subunits that are assembled at the basal end of the growing membrane and are translocated to the apical region of the cells. Both models require the presence of an apical structure in the emerging cells that stabilizes Arm. A good candidate for this function might be the actin network which shows a remarkably similar polarized distribution during cellularization (Warn and Robert-Nicoud, 1990). Apically localized actin may serve to increase stability of cadherin-mediated cell contacts or of junctional precursors in this region. The function of the actin network during cellularization might therefore not be restricted to cytokinesis, but may be required simultaneously for the establishment of apical-basolateral polarity. *Nullo-X* embryos exhibit a highly disorganized actin network during cellularization that can be completely rescued by a *nullo* transgene (Simpson and Wieschaus, 1992). Since such embryos lack X-linked zygotic gene activity other than *nullo*, this result suggests that *sdt* and *baz* are not required for the stability of the actin network, per se.

Although the apical-basolateral axis of the cells is determined early, the final establishment of membrane polarity occurs later. The temporal pattern of Armadillo (Arm) and Neurotactin (NT) distribution during cellularization

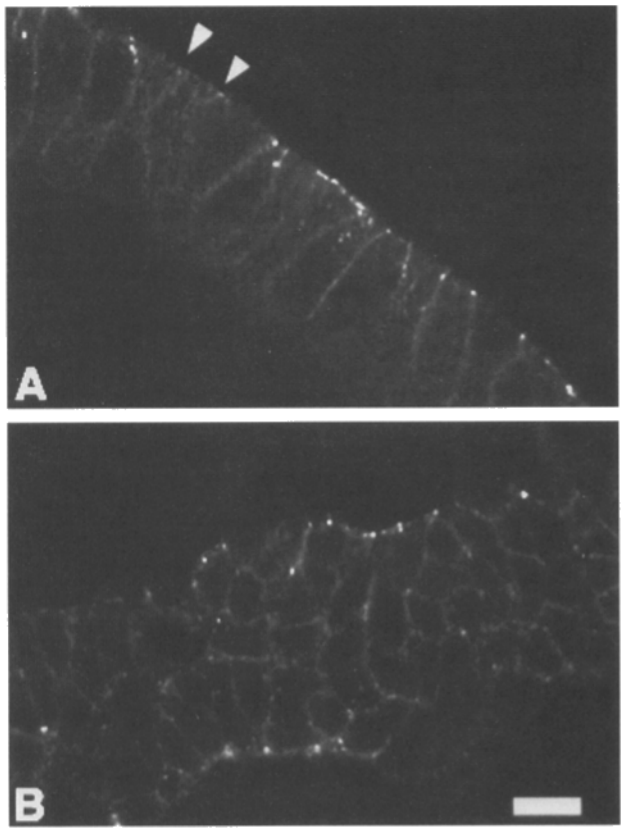

Figure 10. ZA phenotype in embryos missing normal maternal and zygotic Armadillo protein. Germ-line clones of arm^{XP33} were produced as described in Materials and Methods and embryos were fixed and stained for Arm protein. An optical section through the early gastrula (stage 7) is shown in *A* and a slightly older embryo is shown in *B*. The arrowheads in *A* point to lack of apical-lateral localization of Arm at some cell contacts. Note that the monolayered blastoderm epithelium is disturbed in this region. Bar, 10 μm.

and early gastrulation shows dynamic changes until a final separation into three membrane domains is achieved: a basolateral domain (positive for NT), a junctional domain (positive for Arm), and an apical domain (negative for both antigens). The restricted localization of the Crb protein to the apical membrane domain during early gastrulation (stage 6) is consistent with this interpretation (Tepass et al., 1990). The separation into different plasma membrane domains is indicated by the redistribution of apically localized NT to the basolateral domain. This change in NT distribution relative to the forming ZA is a remarkably fast process and may reflect the final step in the establishment of the polarized epithelium. It may either involve a shift of the forming ZA to the apical-lateral border, or a redistribution of NT from the apical to the basolateral domain or both. In any case, it is likely that formation of the polarized epithelium in the ectoderm involves the rapid redistribution of basolateral and junctional membrane proteins.

Cellular Consequences upon Failure to Establish a ZA

According to Tepass and Hartenstein (1994), the development of the typical ZA morphology in the ectoderm is accomplished at the three-layered germ-band stage (stage 11). Incorporating our results into this scheme, we propose three stages in ZA development (Fig. 11): (*1*) a broad apical bias in the distribution of ZA components during cellularization (stage 5); (*2*) the incipient ZA composed of densely aligned spot adherens junctions (SAJs) during and after gastrulation (stages 6 to 10); and (*3*) the continuous beltlike ZA (from stage 11 on). This model of ZA formation raises the question of whether the function of the ZA requires its complete formation.

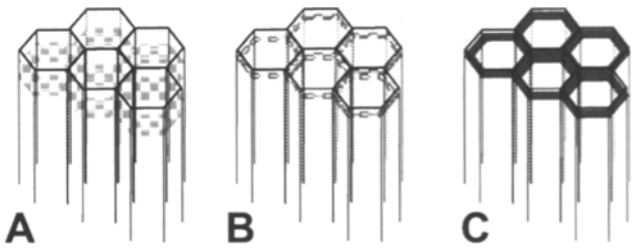

Figure 11. Model for the formation of the ZA in the ectoderm of the developing *Drosophila* embryo. (*A*) During cellularization (stage 5) the distribution of ZA components in the form of preformed spot adherens junctions is biased towards the apical domain of the emerging cells. (*B*) This apical bias leads to the formation of an incipient ZA during gastrulation (stage 6 through 10). The incipient ZA is presumably composed of densely aligned spot adherens junctions that gradually fuse with one another to form a continuous belt adherens junction. (*C*) The classical ZA is fully established after gastrulation (stage 11).

Unlike single mutations that affect epithelial cell polarity in the embryo relatively late, *sdt baz* double mutant embryos exhibit a much earlier phenotype. In *sdt baz* double mutants, the formation of the incipient ZA is inhibited, whereas the formation of the incipient ZA is not affected in *sdt* or *baz* zygotic single mutants (see also Grawe et al., 1996). In addition, the epithelial cells in *sdt baz* mutant embryos undergo profound morphological changes which eventually lead to a complete conversion from a columnar epithelial cell shape to a mesenchymal cell shape. Without any molecular characterization of the products of the genes *sdt* and *baz*, it is difficult to determine whether these two events (i.e., defective incipient ZA and morphological cell shape changes) are causally related to each other. We suspect that these morphological changes are a consequence of the abnormal ZA formation because of two major reasons: (*1*) the ZA defect is a more constant feature that affects all cells in the same manner, while the morphological abnormalities are more variable and often occur later. (*2*) The phenotype of *arm* mutants, in which an adherens junction resident protein is affected, is very similar to the *sdt baz* phenotype. It is also noteworthy in this context that manipulations that interfere with the integrity of the ZA in cultured mammalian epithelial cells lead to a very similar cellular phenotype (i.e., alteration of cell shape, formation of fibroblastoid cells, and development of invasive properties) (Behrens et al., 1989; Reichmann et al., 1992). We therefore propose that the incipient ZAs are functional ZAs, even before they exhibit the continuous beltlike character of mature ZAs at the apical-lateral membrane border.

In the context of morphogenetic movements, the cellular phenotype in *sdt baz* double mutants suggests that the two genes play a role in changing the behavior of epithelial cells. The cell shape changes of some cells in the blastoderm epithelium of *sdt baz* mutant embryos might reflect the initiation of a movement of cells into the interior of the embryo. This movement results in complete multilayering of the originally monolayered epithelium. A similar movement of cells from the surface of an epithelium in the basal direction followed by a transition into mesenchymal cells occurs during gastrulation and is classically described as ingression (Weinberger et al., 1984; Purcell and Keller, 1993). One possible function of *sdt* and *baz* in morphogenesis may be the inhibition of ingression in embryonic epithelia. Local downregulation of *sdt* and *baz* in certain cells within an epithelium might therefore be used to initiate ingression behavior and finally their transition into mesenchymal cells.

A Role for Stardust and Bazooka in the Formation of the Zonula Adherens

The diffuse pattern of Arm during cellularization presumably reflects the presence of spot adherens junctions (SAJ) that have previously been identified by TEM. It has been proposed that the formation of the continuous ZA may require the fusion of SAJs into an apically located belt (Tepass and Hartenstein, 1994). The more lateral position of the SAJs in early embryos mutant for *sdt* and *baz* suggests that the gene products may normally be involved in lateral interactions between SAJs, required for their fusion. In *sdt* single mutants, the number of SAJs is reduced in the early embryo, and a continuous ZA does not form in extended germ-band embryos (stage 10) (Grawe et al., 1996).

A clue as to how ZA assembly might be regulated comes from our observation that embryos which lack the normal maternal and zygotic supply of wild-type *arm* gene product have a similar early phenotype as the *sdt baz* double mutant embryos. The function of Arm in adherens junction formation is also being reported by Cox et al. (1996) with similar results. Taken together, these results suggest that the products of *sdt* and *baz* might be involved in a process which recruits cytoplasmic Arm into the ZA. In this context it is intriguing that embryos mutant for maternal and zygotic *baz* activity (from *baz* germ-line clones) show the same early defect in ZA formation and thus behave similarly to embryos mutant for *arm*. Furthermore, embryos that are only zygotically mutant for *baz* are less severely affected, similar to embryos mutant for zygotic *arm* activity. Further analysis of the *baz* gene is required to determine whether these similarities in the mutant phenotypes of *baz* and *arm* embryos are due to a more direct interaction of the two gene products.

Common or Distinct Pathways for the Establishment of Epithelial Cell Polarity in Drosophila?

The mutations *sdt* and *baz* belong to a group in which mutant embryos show severe abnormalities in the differentiation of the larval cuticle including the genes, *crumbs* (*crb*) and *shotgun* (*shg*) (Jürgens et al., 1984; Nüsslein-Volhart et al., 1984; Wieschaus et al., 1984). Although the similarity in the late phenotypes of these mutants shows that the respective genes are all required for the same process, i.e., epithelial differentiation, it is difficult to determine whether all these genes act in a common pathway. Nevertheless, the genes *crb* and *sdt* show an interesting genetic interaction. Using chromosomal duplications, it has been shown that the phenotype of *crb* (null) mutant embryos can be rescued by an additional copy of *sdt*, but not vice versa (Tepass and Knust, 1993). Based on these findings, a model has been proposed that positions *sdt* downstream of *crb* in a regulatory hierarchy (Tepass and Knust, 1993). This model is complicated by the fact that *sdt* regulates Crb protein distribution (Tepass and Knust, 1993). A more attractive model might be that *sdt* functions in a parallel pathway, and, in sufficient dosage, bypasses the requirement for *crb*.

It is equally complicated to arrange *sdt* and *baz* in a linear pathway given that the double mutant of zygotic null alleles shows a stronger phenotype than the single mutants. The product of the *baz* gene is provided maternally and zygotically (Wieschaus and Noell, 1986). Although maternal *baz* may rescue the hemizygous *baz* phenotype to a certain extent, it is difficult to explain the enhancement of the presumed null phenotype of *sdt* that occurs when *baz* is removed, if the two genes would function in a strictly linear pathway. In summary, we suggest that although *baz*, *crb*, and *sdt* are important for the same process, it is most likely that they act in different, but related pathways.

Although the genes *sdt* and *baz* may prove to be important general regulators in the maintenance of the polarized epithelial cell phenotype, they are certainly not the only genes involved in this process. The present paper presents the first systematic screen to identify the X-linked zygotic requirements for ZA formation in the embryo. It is based on the assumption that the basic components of the ZA are provided maternally, but require a few zygotically active loci to ultimately assemble the ZA. In the case of the X chromosome, the screen revealed two genes, both of which had been found in the mutagenesis screen earlier (Wieschaus et al., 1984). However, expanding our screen to the autosomes has the potential to identify novel, early zygotically active genes required for ZA assembly and epithelial cell polarity.

We thank all members of the Wieschaus and Schüpbach labs for helpful discussions and suggestions during this study. We thank Cynthia Hsuang-Hung for maintaining stocks, Reba Samantha for technical assistance, the Bowling Green Stock Center for providing translocation stocks, the Developmental Studies Hybridoma Bank (Iowa City, IA), and Joe Goodhouse in the EM-Confocal Facility for help with microscopy. We thank Drs. Eli Knust, Helen Skaer, Rachel Cox, and Mark Peifer for communicating results before publication and helpful comments on the manuscript. We are grateful to Yashi Ahmed, Audrey Christiansen, Girish Deshpande, Laura Nilson, Rob Ray, Alain Vincent, and Michael Welte for critically reading the manuscript.

This work has been supported by the Deutsche Forschungs gpmpiuschaft fellowship MU1168/1-1 to H.-A.J. Müller and National Institutes of Health grant 5R01HD22780 to E. Wieschaus.

Received for publication 12 January 1996 and in revised form 17 April 1996.

References

Behrens, J., M.M. Mareel, F. van Roy, and W. Birchmeier. 1989. Dissecting tu-

mor cell invasion: epithelial cells acquire invasive properties after the loss of uvomorulin-mediated cell–cell adhesion. *J. Cell Biol.* 108:2435–2447.
Birchmeier, W., K.M. Weidner, and J. Behrens. 1993. Molecular mechanisms leading to loss of differentiation and gain of invasiveness in epithelial cells. *J. Cell Sci. Suppl.* 17:159–164.
Chou, T.-B., and N. Perrimon. 1992. Use of a yeast site-specific recombinase to produce female germline chimeras in *Drosophila*. *Genetics.* 131:906–916.
Collins, J., and T.P. Fleming. 1995. Epithelial differentiation in the mouse preimplantation embryo: making adhesive contacts for the first time. *Trends Biochem. Sci.* 20:307–312.
Cox, R., C. Kirkpatrick, and M. Peifer. 1996. Armadillo is required for adherens junction assembly, cell polarity and morphogenesis during *Drosophila* embryogenesis. *J. Cell Biol.* In press.
Eaton, S., and K. Simons. 1995. Apical, basal, and lateral cues for epithelial polarization. *Cell.* 82:5–8.
Eichenberger-Glinz, S. 1979. Intercellular junctions during development and in tissue cultures of *Drosophila melanogaster*: an electron-microscopic study. *Roux Arch. Dev. Biol.* 186:333–349.
Fleming, T.P., and M.H. Johnson. 1988. From egg to epithelium *Annu. Rev. Cell Biol.* 4:459–485.
Fleming, T.P., Q. Javed, J. Collins, and M. Hay. 1993. Biogenesis of structural intercellular junctions during cleavage in the mouse embryo. *J. Cell Sci. Suppl.* 17:119–125.
Garrod, D.R., and J.E. Collins. 1992. Intercellular junctions and cell adhesion in epithelial cells. *In* Epithelial Organization and Development. T.P. Fleming, editor. Chapman and Hall, London. pp. 1–52.
Geiger, B., and D. Ginsberg. 1991. The cytoplasmic domain of adherens junctions. *Cell Motil. Cytoskeleton.* 20:1–6.
Grawe, F., A. Wodarz, B. Lee, E. Knust, and H. Skaer. 1996. The *Drosophila* genes *crumbs* and *stardust* are involved in the biogenesis of adherens junctions. *Development.* 122:951–959.
Gumbiner. B., B. Stevenson, and A. Grimaldi. 1988. The role of the cell adhesion molecule uvomorulin in the formation and maintenance of the epithelial junctional complex. *J. Cell Biol.* 107:1575–1587.
Hortsch, M., N.H. Patel, A.J. Bieber, Z.R. Traquina, and C.S. Goodman. 1990. *Drosophila* neurotactin, a surface glycoprotein with homology to serine esterases, is dynamically expressed during embryogenesis. *Development.* 110: 1327–1340.
Jürgens, G., E. Wieschaus, C. Nüsslein-Volhart, and H. Kluding. 1984. Mutations affecting the pattern of the larval cuticle in *Drosophila melanogaster*: II. Zygotic loci on the third chromosome. *Roux Arch. Dev. Biol.* 193:283–295.
Kemler, R. 1993. From cadherins to catenins: cytoplasmic protein interactions and regulation of cell adhesion. *Trends Genet.* 9:315–320.
Kirkpatrick, C., and M. Peifer. 1995. Not just glue: cell–cell junctions as cellular signaling centers. *Curr. Opin. Gen. Dev.* 5:56–65.
Knust, E. 1994. Control of epithelial cell polarity in *Drosophila*. *Trends Genet.* 10:275–280.
Knust, E., U. Tepass, and A. Wodarz. 1993. *crumbs* and *stardust*, two genes of *Drosophila* required for the development of epithelial cell polarity. *Development Suppl.* :261–268.
Lane, N.J., and H.I. Skaer. 1980. Intercellular junctions in insect tissues. *Adv. Insect Physiol.* 15:35–213.
Larue, L., M. Ohsugi, J. Hirchenhain, and R. Kemler. 1994. E-Cadherin null mutant embryos fail to form a trophectoderm epithelium. *Proc. Natl. Acad. Sci. USA.* 91:8263–8267.
Lentz, T.L., and J.P. Trinkaus. 1967. A fine-structural study of cytodifferentiation during cleavage, blastula, and gastrula stages of *Fundulus heteroclitus*. *J. Cell Biol.* 32:121–138.
Magee, A.I., and R.S. Buxton. 1991. Transmembrane molecular assemblies regulated by the greater cadherin family. *Curr. Opin. Cell. Biol.* 3:854–861.
Mahowald, A.P. 1963. Electron microscopy of the formation of the cellular blastoderm in *Drosophila melanogaster*. *Exp. Cell Res.* 32:457–468.
Mays, R.W., K.A. Beck, and W.J. Nelson. 1994. Organization and function of the cytoskeleton in polarized epithelial cells: a component of the protein sorting machinery. *Curr. Opin. Cell Biol.* 6:16–24.
McNeill, H., and W.J. Nelson. 1992. Shaping an epithelial cell: the role of cell adhesion molecules in the reorganization of the membrane cytoskeleton. *In* Epithelial Organization and Development. T.P. Fleming, editor. Chapman and Hall, London. 53–88.
McNeill, H., M. Ozawa, R. Kemler, and W.J. Nelson. 1990. Novel function of the cell adhesion molecule uvomorulin as an inducer of cell polarity. *Cell.* 62: 309–316.
McNeill, H., T.A. Ryan, S.J. Smith, and W.J. Nelson. 1993. Spatial and temporal dissection of immediate and early events following cadherin mediated epithelial cell adhesion. *J. Cell Biol.* 120:1217–1226.
Mege, R.-M., F. Matsuzaki, W.J. Gallin, J.I. Goldberg., B.A. Cunningham, and G.M. Edelman. 1988. Construction of epitheloid sheets by transfection of mouse sarcoma cells with cDNAs for chicken cell adhesion molecules. *Proc. Natl. Acad. Sci. USA.* 85:7274–7278.
Miller, K.G., C.M. Field, and B.M. Alberts. 1989. Actin-binding proteins from *Drosophila* embryos: a complex network of interacting proteins detected by F-actin affinity chromatography. *J. Cell Biol.* 109:2963–2975.
Müller, H.-A.J., and P. Hausen. 1995. Epithelial cell polarity in early *Xenopus* development. *Dev. Dyn.* 202:405–420.
Naethke, I.S., L.E. Hinck, and W.J. Nelson. 1993. Epithelial cell adhesion and development of cell surface polarity: possible mechanism for modulation of cadherin function, organization and distribution. *J. Cell Sci. Suppl.* 17:139–145.
Nelson, W.J. 1992. Regulation of cell surface polarity from bacteria to mammals. *Science (Wash. DC).* 258:948–955.
Nüsslein-Volhart, C., E. Wieschaus, and H. Kluding. 1984. Mutations affecting the pattern of the larval cuticle in *Drosophila melanogaster*: I. Zygotic loci on the second chromosome. *Roux Arch. Dev Biol.* 193:267–282.
Oda, H., T. Uemura, K. Shiomi, A. Nagafuchi, S. Tsukita, and M. Takeichi. 1993. Identification of a *Drosophila* homologueue of α-catenin and its association with the Armadillo protein. *J. Cell Biol.* 121:1133–1140.
Oda, H., T. Uemura, Y. Harada, Y. Iwai, and M. Takeichi. 1994. A *Drosophila* homologue of cadherin associated with Armadillo and essential for embryonic cell–cell adhesion. *Dev. Biol.* 165:716–726.
Peifer, M. 1993. The product of the *Drosophila* segment polarity gene *armadillo* is part of a multi-protein complex resembling the vertebrate adherens junction. *J. Cell Sci.* 105:993–1000.
Peifer, M. 1995. Cell adhesion and signal transduction: the Armadillo connection. *Trends Cell Biol.* 5:224–229.
Peifer, M., and E. Wieschaus. 1990. The segment polarity gene *armadillo* encodes a functionally modular protein that is the *Drosophila* homologue of human plakoglobin. *Cell.* 63:1167–1178.
Peifer, M., S. Orsulic, D. Sweeton, and E. Wieschaus. 1993. A role of the *Drosophila* segment polarity gene *armadillo* in cell adhesion and cytoskeletal integrity during oogenesis. *Development.* 118:1191–1207.
Peifer, M., D. Sweeton, M. Casey, and E. Wieschaus. 1994. *Wingless* signal and Zeste-white 3 kinase trigger opposing changes in the intracellular distribution of Armadillo. *Development.* 120:369–380.
Purcell, S., and R. Keller. 1993. A different type of amphibian mesoderm morphogenesis in *Ceratophrys ornata*. *Development.* 117:307–317.
Ranscht, B. 1994. Cadherins and catenins: interactions and functions in embryonic development. *Curr. Opin. Cell Biol.* 6:740–746.
Reichmann, E., H. Schwarz, E.-M. Deiner, I. Leitner, M. Eilers, J. Berger, M. Busslinger, and H. Beug. 1992. Activation of an inducible c-FosER fusion protein causes loss of epithelial polarity and triggers epithelial-fibroblastoid cell conversion. *Cell.* 71:1103–1116.
Reynolds, A.B., J. Daniel, P.D. McCrea, M.J. Wheelock, J. Wu, and Z. Zhang. 1994. Identification of a new catenin: the tyrosine kinase substrate $p120^{cas}$ associates with E-cadherin complexes. *Mol. Cell Biol.* 14:8333–8342.
Riethmacher, D., V. Brinkmann, and C. Birchmeier. 1995. A targeted mutation in the mouse E-cadherin gene results in defective preimplantation development. *Proc. Natl. Acad. Sci. USA.* 92:855–859.
Riggleman, B., P. Schedl, and E. Wieschaus. 1990. Spatial expression of the *Drosophila* segment polarity gene *armadillo* is posttranscriptionally regulated by *wingless*. *Cell.* 63:549–560.
Rodriguez-Boulan, E., and W.J. Nelson. 1989. Morphogenesis of the polarized epithelial cell phenotype. *Science (Wash. DC).* 245:718–725.
Sanders, E.J. 1975. Aspects of furrow membrane formation in the cleaving *Drosophila* embryo. *Cell Tiss. Res.* 156:463–474.
Schejter, E.D., and E. Wieschaus. 1993. Functional elements of the cytoskeleton in the early *Drosophila* embryo. *Annu. Rev. Cell Biol.* 9:67–99.
Shiel, M., and M.J. Caplan. 1995*a*. The generation of epithelial polarity in mammalian and *Drosophila* embryos. *Semin. Cell Biol.* 6:39–46.
Shiel, M., and M.J. Caplan. 1995*b*. Developmental regulation of membrane protein sorting in *Drosophila* embryos. *Am. J. Physiol.* 296:C207–C216.
Simons, K., and S.D. Fuller. 1985. Cell surface polarity in epithelia. *Annu. Rev. Cell Biol.* 1:243–288.
Simpson, L., and E. Wieschaus.1990. Zygotic activity of the *nullo* locus is required to stabilize the actin-myosin network during cellularization in *Drosophila*. *Development.* 110:851–863.
Simpson, L., and E. Wieschaus. 1992. The *Drosophila* cellularization gene *nullo* produces a blastoderm-specific transcript whose levels respond to the nucleocytoplasmic ratio. *Genes Dev.* 6:1255–1268.
Staehelin, L.A. 1974. Structure and function of intercellular junctions. *Int. Rev. Cytol.* 39:191–283.
Takata, K., and S.J. Singer. 1988. Phosphotyrosine-modified proteins are concentrated at the membranes of epithelial and endothelial cells during tissue development in chick embryos. *J. Cell Biol.* 106:1757–1764.
Takeichi, M. 1993. Cadherins in cancer: implications for invasion and metastasis. *Curr. Opin. Cell Biol.* 5:806–811.
Tepass, U., and E. Knust. 1993. *crumbs* and *stardust* act in a genetic pathway that controls the organization of epithelia in *Drosophila melanogaster Dev. Biol.* 159:311–326.
Tepass, U., and V. Hartenstein. 1994. The development of cellular junctions in the *Drosophila* embryo. *Dev. Biol.* 161:563–596.
Tepass, U., C. Theres, and E. Knust. 1990. *crumbs* encodes an EGF-like protein expressed on apical membranes of *Drosophila* epithelial cells and required for organisation of epithelia. *Cell.* 61:787–799.
Trelstad, R.L., E.D. Hay, and J.P. Revel. 1967. Cell contact during early morphogenesis of the chick embryo. *Dev. Biol.* 16:78–106.
Tsukita, S., S. Tsukita, A. Nagafuchi, and S. Yonemura. 1992. Molecular linkage between cadherins and actin filaments in cell-cell adherens junctions. *Curr. Opin. Cell Biol.* 4:834–839.
Vestweber, D., and R. Kemler. 1984. Rabbit antiserum against a purified cell

surface glycoprotein decompacts mouse preimplantation embryos and reacts with specific adult tissues. *Exp. Cell Res.* 152:169–178.

Warn, R.M., and M. Robert-Nicoud. 1990. F-Actin organization during the cellularization of the *Drosophila* embryo as revealed with a confocal laser scanning microscope. *J. Cell Sci.* 96:35–42.

Weinberger, C., P.L. Penner, and I. Brick. 1984. Polyingression, an important morphogenetic movement in chick gastrulation. *Am. Zool.* 24:545–554.

Wieschaus, E., and E. Noell. 1986. Specificity of embryonic lethal mutations in *Drosophila* analyzed in germ line clones. *Roux Arch. Dev. Biol.* 195:63–73.

Wieschaus, E., and D. Sweeton. 1988. Requirements for X-linked zygotic gene activity during cellularization of early *Drosophila* embryos. *Development.* 104:483–493.

Wieschaus, E., C. Nüsslein-Volhart, and G. Jürgens. 1984. Mutations affecting the pattern of the larval cuticle in *Drosophila melanogaster* III. Zygotic loci on the X chromosome and the fourth chromosome. *Roux Arch. Dev. Biol.* 193:296–307.

Wodarz, A., F. Grawe, and E. Knust. 1993. CRUMBS is involved in the control of apical protein targeting during *Drosophila* epithelial development. *Mech. Dev.* 44:175–187.

Wodarz, A., U. Hinz, M. Engelbert, and E. Knust. 1995. Expression of Crumbs confers apical character on plasma membrane domains of ectodermal epithelia of *Drosophila*. *Cell.* 82:67–76.

Woods, D.F., and P.J. Bryant. 1993. Apical junctions and cell signalling in epithelia. *J. Cell Sci. Suppl.* 17:171–181.